

Catalysis Science & Technology

Accepted Manuscript



This article can be cited before page numbers have been issued, to do this please use: R. BAL, N. Siddiqui, B. Sarkar, C. Pendem, R. khatun, K. S. L. N., A. Bordoloi and T. Sasaki, *Catal. Sci. Technol.*, 2017, DOI: 10.1039/C7CY00989E.



This is an Accepted Manuscript, which has been through the Royal Society of Chemistry peer review process and has been accepted for publication.

Accepted Manuscripts are published online shortly after acceptance, before technical editing, formatting and proof reading. Using this free service, authors can make their results available to the community, in citable form, before we publish the edited article. We will replace this Accepted Manuscript with the edited and formatted Advance Article as soon as it is available.

You can find more information about Accepted Manuscripts in the [author guidelines](#).

Please note that technical editing may introduce minor changes to the text and/or graphics, which may alter content. The journal's standard [Terms & Conditions](#) and the ethical guidelines, outlined in our [author and reviewer resource centre](#), still apply. In no event shall the Royal Society of Chemistry be held responsible for any errors or omissions in this Accepted Manuscript or any consequences arising from the use of any information it contains.



Journal Name

ARTICLE

Highly selective transfer hydrogenation of α,β -unsaturated carbonyl compounds using Cu based nanocatalysts†

Received 00th January 20xx,

Accepted 00th January 20xx
DOI: 10.1039/x0xx00000x

www.rsc.org/

Nazia Siddqui,^a Bipul Sarkar,^{a,b} Chandrashekar Pendem,^a Rubina khatun^a, L.N. Sivakumar Konthala,^a Takehiko Sasaki,^c Ankur Bordoloi^a and Rajaram Bal*^a

Simultaneous dehydrogenation of cyclohexanol to cyclohexanone and hydrogenation of α,β unsaturated carbonyl compounds to corresponding α,β unsaturated alcohols was carried out in a single pot reaction (Scheme 1) without addition of any external hydrogen donor. Cu nanoclusters supported on nanocrystalline MgO was found to be the active catalyst for the chemoselective transfer hydrogenation of unsaturated carbonyl compounds to produce corresponding alcohols with very high yield. Transfer hydrogenation of cyclohexanol and cinnamaldehyde produce cyclohexanone and cinnamyl alcohol with 100% selectivity. This Cu/MgO catalyst can be easily recovered and recycled up to more than five times without any significant loss of activity which confirmed the true heterogeneous nature of the catalyst. Several α,β unsaturated compounds were also tested for this reaction and found that all the cases the yields is > 95%. The ease in handling without requiring high pressure H₂ or hazardous hydrogen source make this transfer hydrogenation more practical and useful.

Introduction

The future demand for hydrogen as an energy source will tremendously increase due to the worldwide shortage of fossil resources. Therefore researchers are working for new process to save H₂ as a feedstock in chemical processes which are currently consuming 50% of the total H₂ reverence. So an innovative and unexplored approach will be the coupling of dehydrogenation reaction with a hydrogenation reaction. Thus the transfer (de) hydrogenation of alcohols by aldehydes and ketones would be an effective way of high H₂ and energy economy, since no external H₂ supply is required and the energy is saved due to the coupling of endothermic dehydrogenation with exothermic hydrogenation.¹⁻³

The selective hydrogenation of α,β Unsaturated aldehydes and ketones to corresponding unsaturated alcohols is of paramount importance in organic synthesis.¹ These unsaturated alcohols are intermediates used in the production of foods, pharmaceuticals and cosmetics.^{4, 5} The hydrogen addition to the conjugated C=C bond in an α,β unsaturated carbonyl compounds is both kinetically and thermodynamically favoured over C=O.⁶ Therefore research efforts have been made for improving the selectivity of unsaturated alcohols. Industrially, hydrogenation of α,β -unsaturated carbonyls have been

achieved using stoichiometric amounts of reducing agents such as metal hydrides (LiAlH₄, NaBH₄ etc).⁷ Apart from environmental problem, the use of halides as base is also associated with corrosion problem. Additionally, the reducing agents used in this process are used in stoichiometric condition and required careful handling under anhydrous condition. Although, substantial efforts have been made for the selective reduction of C=O group of the unsaturated aldehydes and ketones but the development of truly heterogeneous catalyst still remains a challenges for the researchers. Different Nobel metals like Pt,⁸ Pd,⁹ Ru,¹⁰ Rh,¹¹ Ir,¹² and Au¹³ have been used for the selective hydrogenation of C=O bond in α,β unsaturated aldehydes and ketones to achieve high yield. It has been reported in the literature that the selectivity of unsaturated alcohols can be enhanced by using different catalyst supports,⁸ promoters,¹⁰ controlling the particle size,¹⁴ doping of secondary metal.¹⁵ As these metals are very expensive with low abundance, researchers are looking for cheaper metals for practical use in industry. Supported nickel and copper catalysts can be used for this selective hydrogenation reaction due to its lower price and its selective hydrogenation property.^{16, 17} Among different hydrogenation methods, catalytic transfer hydrogenation have potential advantages over the reduction using molecular hydrogen or any other H-donors like LiAlH₄, NaBH₄ etc. We report here the preparation of Cu-nanoparticles supported on nanocrystalline MgO for selective hydrogenation of α,β -unsaturated carbonyl compounds to corresponding α,β -unsaturated alcohols.

Dehydrogenation of cyclohexanol to cyclohexanone a very important industrial process for the production of nylon as two major raw materials caprolactum and adipic acid are obtained from cyclohexanone. Cyclohexanone is also used as a solvent in different coating processes. This dehydrogenation reaction is

^a Refinery Technology Division, CSIR- Indian Institute of Petroleum, Dehradun-248005, UK, India, E-mail: raja@iip.res.in

^b SKKU Advanced Institute of Nano Technology, Sungkyunkwan University, Republic of Korea

^c Department of Complexity Science and Engineering, Graduate School of Frontier Sciences, The University of Tokyo, Kashiwanoha, Kashiwa-shi, Chiba 277-8561, Japan
Electronic Supplementary Information (ESI) available: [details of any supplementary information available should be included here]. See DOI: 10.1039/x0xx00000x

endothermic ($\Delta H=65$ KJ/mol) and thermodynamically reversible.¹⁸ This combine effect of endothermic nature for minimum energy usage has directed the researchers for searching a promising catalyst that can be used at lower temperatures. Several Cu based catalysts have been tried for this reaction but it was found that lower temperatures (150°C-300°C), the cyclohexanone yield is very low and at higher temperatures (350°C-450°C) catalysts deactivates easily.⁸

Copper based catalysts have unique performance for selective hydrogenation of rapeseed oils.¹⁹ In situ reduced Cu catalysts supported on Fe₂O₃ catalyst has been reported for the transfer hydrogenation or hydrogenolysis of furanic aldehydes, utilizing alcohols as hydrogen donors.²⁰ Hansen *et al.* used Cu-doped porous metal oxide in supercritical methanol for one-pot reduction of 5-hydroxymethylfurfural to DMF.²¹

Choice of support is also a key parameter which could influence the selectivity towards carbonyl bond hydrogenation through metal-support interaction. Typical supports used in chemoselective hydrogenation of α,β -unsaturated carbonyl compounds are metal oxides, such as acidic Al₂O₃,²² SiO₂,²³ TiO₂¹⁰ and basic MgO.¹⁰ Acidic support (like Al₂O₃) provide the electron-deficient surface metallic counterpart, which enhanced the adsorption of H₂, so rapid hydrogenation takes place²⁴

We report here the preparation of Cu-MgO catalyst via sonication method and this prepared catalyst is highly active for the chemo-selective transfer hydrogenation of α,β unsaturated carbonyl compounds to corresponding α,β -unsaturated alcohols. To best of our knowledge there is no report in the open literature where a single heterogeneous catalyst is used for the dehydrogenation of cyclohexanol to cyclohexanone where this in-situ generated hydrogen is used for selective hydrogenation of α,β unsaturated aldehydes and ketones to unsaturated alcohols.

Experimental

Materials

Magnesium nitrate hexahydrate (99%), Copper nitrate hemipenta hydrate, hydrazine (80% aq. solution), were purchased from Sigma-Aldrich Co. Cinnamaldehyde, citral, crotonaldehyde and its all derivatives were purchased from Merck KGaA, Darmstadt, Germany. All the chemicals were used without further purification and addition.

Catalyst Synthesis

Well dispersed nanocrystalline copper oxide supported on magnesia (Cu/MgO) was prepared by simple ultra-sonication assisted synthesis procedure. In a typical synthesis, 16.0 g of Mg(NO₃)₂·6H₂O was dissolve in 100 ml of deionised water in 250 ml round bottom flask under vigorous stirring. 0.23g of Cu(NO₃)₂·2.5H₂O, was added dropwise to the above solution with constant stirring. The suspension was kept for 30 min followed by ultra-sonication. 50ml of 1M Na₂CO₃ solution was added dropwise in to the above mixture during sonication and the pH of the mixture was adjusted to ~9. After 2h sonication, few drops of hydrazine was added and sonicated for additional 1 h. The suspension was kept overnight for further aging followed by filtration and washed with hot water and dried at

100°C for 6h. The powdered material was finally calcined at 550°C for 6h.

Reduction of Aldehydes and ketones

The transfer hydrogenation reactions were performed in a high-pressure batch reactor (Parr made) equipped with a magnetically driven stirrer. Typically, the substrate, catalyst, and cyclohexanol was mixed in the reactor and stirred for 15 min at room temperature. The system was purged with N₂ twice to remove air and the pressure was increased up to 1MPa. Prior to each experiment, the catalyst (0.1 g) was reduced at 350°C for 2 h with H₂ (10% H₂ balance He). Aliquots were withdrawn through the special sample port attached within the reactor. At the end of reaction, the reactor was cooled down to room temperature and then pressure was released very slowly. The catalyst particles was separated by centrifuging and the reaction products were identified by GC-MS (HP 5890 GC coupled with 5972 MSD). The identified product was analysed in a Thermo GC 700, fitted with a HP-5 (30m X 0.28mm i. d., 0.25 μ m film thickness) capillary column and a FID detector.

The recyclability of the catalyst was tested by separating it from the reaction system by centrifugation, washing the catalyst with water and ethanol, followed by drying at 90°C for overnight. In the recyclable test of Cu-MgO, the Cu concentration in the filtrate was less than 2 ppb as confirmed by ICP analysis after separating the spent catalyst, indicating that no Cu leaching occurred during the reaction.

Catalyst Characterization

Powder x-ray diffraction (XRD) measurements were performed with a Bruker D8 advance x-ray diffractometer with a Cu K α radiation (40 kV and 30 mA) in the 2 θ range 5-60°. The SEM images are taken on a FEI Quanta 200 F, using ETD detector with an acceleration tension of 10 or 30 kV. All the Samples were analyzed by spreading them on a carbon tape and coated with gold to increase the electrical conductivity. Energy dispersive X-ray spectroscopy (EDX) was used in connection with SEM for the elemental analysis. The elemental mapping was also collected with the same spectrophotometer. The morphology, lattice fringes and crystal boundaries of the samples were examined using a JEOL JEM 2100 high-resolution transmission electron microscope (HRTEM). X-Ray photoelectron spectra (XPS) of the catalysts were recorded with a Thermo Scientific K-Alpha X-Ray photoelectron equipped with Mg K α radiation. The C 1s peak at 284.8 eV was used as a calibration peak. Temperature programmed reduction (TPR) and Temperature programmed desorption (TPD) experiments were carried out in a Micromeritics, Auto Chem II 2920 instrument connected with a thermal conductivity detector (TCD). Prior to TPR, the catalysts were also heated at 650°C for 2 h in helium and then placed in 10% H₂/Ar with a flow rate of 40 mL min⁻¹ in the temperature range of 40-1000 °C with an increment of 10 °C/min. The amount and strength of the basic site were measured by CO₂ adsorption-desorption technique using the same Micromeritics, Auto Chem II 2920 instrument. About 0.1 g sample was saturated with CO₂ at 100°C and flashed with He to remove the physically adsorbed CO₂, finally the decomposition of NH₃ was carried at a heating rate of 10°C/ min under, He flow.

Extended X-ray absorption fine structure spectroscopy (XAFS) measurements of Cu-K edge were carried out at the High Energy Accelerator Research Organization (KEK-IMMS-PF), Tsukuba, Japan. The EXAFS spectrum of the fresh catalyst was measured in the transition mode, whereas for the spent catalyst the EXAFS spectrum was measured in the fluorescence mode using a Lytle detector with Ar gas and spectra were taken at BL-7C and BL-9C at the Photon Factory, Tsukuba, Japan. The electron storage ring was operated at 2.5 GeV and 450 mA; synchrotron radiation from the storage ring was monochromatized by a Si(111) channel cut crystal. Ionized chamber, which were used as detectors for incident X-ray (I_0) and transmitted X-ray (I), were filled with N_2 mixture gas, respectively. The angle of the monochromators was calibrated with Co foil. The EXAFS raw data was analysed with UWXAFS analysis package²⁵ including background subtraction program AUTOBK²⁶ and curve fitting program FEFFIT.²⁷ The amplitude reducing factor, S_0^2 was fixed at 1.0. The backscattering amplitude and phase shift were calculated theoretically by FEFF 8.4 code.²⁸ ATOMS²⁹ were used to obtain FEFF input code for crystalline materials. The angle of the monochromators was calibrated with Cu foil.

Results and discussion

The powder x-ray diffraction (XRD) pattern of 5%Cu-MgO catalysts is shown in Figure 1. The standard diffraction patterns for Cu_2O and CuO are also shown as references. All the Cu-MgO catalyst exhibited the characteristics peaks at 2θ values of 36.9, 42.9, 62.3, 74.7 and 78.6, which corresponds to the (111), (200), (220), (311), and (222) planes of cubic MgO as confirmed by JCPDS card 01-1235. In the diffraction pattern of MgO, the peak at 2θ value of 48.7° which corresponds to $Mg(OH)_2$ was also detected³⁰ This is probably because of the hydroscopic nature of the materials or inherent moisture. For 5%Cu-MgO, (Figure 1e) the diffraction peak at 48.8° correspond to the presence of metallic Cu³¹ indicating the partial reduction of Cu ion during synthesis and calcination. In XRD pattern along with the presence of Cu⁰, (JCPDS card no 04-0836) the soldered peak at 42.1° also indicates the presence of CuO within the catalyst. For the used catalyst (Figure 1f) the intensity of the peak corresponds to metallic Cu⁰ reduced significantly, whereas the intensity of CuO peak increases. This observation clearly indicates the oxidation of Cu⁰ to Cu⁺² during the reaction. BET surface area (Table 1) of the Cu-MgO catalyst increases compare to MgO alone when 2.5% Cu was loaded on it. We believe that ultrasonic treatment during the preparation procedure helps to create additional pores with low loading Cu. It was also observed that with the increase in Cu loading, the pores get blocked by the Cu species and the surface area was decreased (Figure 1). The H_2 pulse chemisorption was done to calculate the dispersion of Cu over MgO support. 2.5%Cu-MgO catalyst shows 27.5% Cu dispersion which reaches the maxima to 49.7%, when Cu loading was 5% then the dispersion decreased with further increases Cu content which may be due to the rapid agglomeration caused with higher Cu loading.³² The amount of Cu and MgO present in the sample was estimated by ICP-AES. The SEM images of fresh and spent catalysts are identical showing that there is no change in morphology (shown in ESI

Figure S1-S3). The TEM image of the Cu-MgO catalyst is shown in (Figure 2). The TEM images (Figure 2a, b) shows spherical nature of MgO particles with size about 30-50 nm. The Cu particles size distribution histogram is also presented in Figure 2a. The distribution histogram shows that the average particle size is about 12nm. The lattice fringes with d-spacing of 0.189nm corresponding to the [111] plane of Cu with a diffraction angle (43.6°) are also presented. The selected area electron diffraction is also represented in fig. 2c and 2d from where the diffraction planes for Cu and MgO was clearly visible.

The TPR profile of prepared Cu-MgO catalysts are shown in Figure 3. MgO has very high reduction potential (E° -2.372V) which makes it hard to reduce, thus no reduction peak is observed for MgO.³³ The TPR profile of 5%Cu-MgO was characterized by a single symmetric peak with the main reduction peak (T_{max}) appeared at $214^\circ C$. The presences of single symmetric peak without any shoulder peak indicates the single stage reduction of CuO to Cu^0 . On the other hand, for Cu-MgO catalysts prepared by using hydrazine and with prolonged sonication time, the TPR peaks (T_{max}) were shifted to higher temperatures. This result indicates that due to the increase in particle size T_{max} increases and the same observation was experienced in our previous studies also^{34,35} With increase in Cu particle size the reduction behaviour of core Cu- species increases and it takes more time and temperature to reduce the Cu particles.³⁰ Generally, the reduction of large Cu-species will be inhibited by the less exposure of the core Cu-species due to agglomeration of Cu species which inhibits the reduction of core Cu species of copper oxide particles by the diffusion of hydrogen molecules, as the core species are not readily exposed to the hydrogen for reduction.³⁶ Thus we attributed the symmetric peak at $214^\circ C$ (Figure 3d) for to the reduction of very small copper oxide nanoclusters.³⁶ Type of basic site and amount of basicity of various Cu-MgO catalyst was measured using CO_2 -TPD and shown in Figure 4 and Table 1. The TPD profile of the Cu-MgO catalyst shows the presence of moderate basic sites within the catalyst. While, the peak position shift to lower value (i.e. toward weak basicity) with the increase in metal loading (Figure 4). On the other side the amount of total basicity (in mmol/g) appears to fall down with the metal loading. This result appears well in agreement with the reported literature.³⁷ The representative XPS spectra of the Cu-MgO catalyst are shown in Figure 5. On deconvolution, the Cu 2p XPS spectra (Figure 5) for the fresh 5%Cu-MgO catalyst shows two different type of Cu species. The peak at binding energy (BE) value of 934.3 eV with strong satellite corresponds to the presence of Cu⁺² species was observed, whereas the peak at 933.0 eV may be attributed to the presence of either Cu⁺¹ or Cu⁰.^{35, 38} In accordance to the Augur spectra (shown in Figure 5) we identified the presence of Cu⁰ in our catalyst. For the spent catalyst, we experienced only Cu⁰ species at BE value of 933.0 eV. Thus we believe that metallic Cu is the active species during the reaction. The XPS spectra for Mg 2p showed the presence of pure MgO at BE value of 51.1 eV for the fresh and spent catalyst. The FT-IR spectrum (Figure 6) of Cu-MgO (uncalcined) shows a strong absorption at 530, 1182 and 1440 cm^{-1} , which is due to

the Mg-O interactions^{39, 40} Whereas, the peak observed at 3432 cm^{-1} corresponds to the O-H stretching vibration. The spectra in the $\nu(\text{OH})$ region shows two bands at 1480 and 1638 cm^{-1} ; corresponds to the O-H bending mode present in the catalyst.⁴¹ Furthermore, the thermal behaviour of the 5%Cu-MgO (uncalcined) samples are studied by TGA/DTA analysis as shown in Figure 7 in the temperature range of RT-900°C. A low temperature endotherm in the 90-120°C region corresponds to the weight loss for physisorbed water molecule by the catalyst. Whereas, the weight loss in the region 150-250° associated with the removal of chemisorbed water molecules associated with Cu and Mg cations. As water has higher affinity with Mg cations thus the volume of chemisorb water is more than physisorbed water molecule. The weight loss in the far end (in the region 380-520°C) can be assigned for the loss of carbonate⁴² used during the sonication.

Detailed structural parameters of the Cu species were obtained by Cu K-edge EXAFS analysis and the curve fitting results are summarized in Table 2. The fresh and spent 5%Cu-MgO catalysts show the presence of CuO (as Cu-O path) clusters. In addition, the spent catalyst showed the formation of metallic Cu (as Cu-Cu path) clusters and we believed that this metallic Cu nanoclusters species are the active species for this reaction. The Cu-O coordination number (CN) in the fresh catalyst was 2.0 ± 0.4 and the Cu-O distance was $1.958 \pm 0.012 \text{ \AA}$, which is similar to the bond length of CuO oxide.³⁵ The small CN of Cu-O indicates the formation of nanosized CuO on the MgO surface. The EXAFS data for the spent catalyst indicate no significant change in CuO structures during the catalysis (Table 2). The Fourier transform Cu K-edge EXAFS spectra for the fresh and spent $1.958 \pm 0.012 \text{ \AA}$ are shown in Figure S4, in supporting information.

Hydrogenation of cinnamaldehyde employing different H₂ donor

Table 2 shows the hydrogenation activity of cinnamaldehyde in presence of different H₂ donor groups. In general, at high temperature (well above of boiling point), especially in presence of catalyst, almost any alcohol can donate hydrogen.⁴³ Thereby, we got considerable conversion of cinnamaldehyde in all the cases (entry 1-4) with 100% cinnamyl alcohol selectivity. As cyclohexanol have relatively low oxidizing potential ($E_{\text{p}2}$) of $>2.0 \text{ V}$ ⁴⁴ compare to 2-butanol and iso-propanol (IPA). Thus, we experience highest conversion of cinnamaldehyde (97.2%) with 100% cinnamyl alcohol selectivity. It is also to note that that cyclohexanol can donate sufficient amount of H₂ under relatively less temperature than other H₂ donor compounds (entry 1-4) in presence of Cu-MgO. Furthermore, we extend our study over different Cu-MgO catalyst prepared by conventional deposition methods along with commercial MgO and CuO and the results are listed in Table S1 (in supporting information). Commercial MgO, CuO (form Sigma Aldrich) and MgO prepared by sonochemical method did not show any activity. Cu-MgO prepared by conventional impregnation (Cu-MgO^{imp}) and co-precipitation (Cu/MgO^{co-pre}) also showed low activity, in compare, Cu-MgO (catalyst prepared by sonochemical method) showed very high activity toward cinnamaldehyde hydrogenation. The results can be explained by the metal

dispersion achieved for all the catalyst as shown in Table 1. It can be noted, that sonochemical approach achieved 49.7% metal dispersion (MD) with Cu specific surface are of $336.6 \text{ m}^2 \text{ g}^{-1}$; whereas catalyst prepared by conventional method shows poor MD with low Cu specific surface between $77.2\text{-}29.2 \text{ m}^2 \text{ g}^{-1}$. Thereby, it can be concluded narrow particle size with higher Cu dispersion of 5%Cu-MgO is the key factor for the high catalytic activity. The reuseability of 5%Cu-MgO catalyst was also tested by conducting four consecutive runs with the same catalysts and the data is tabulated in Table S1 and Figure S5. 100% selectivity was found even after four reuses whereas, the conversion drop by 0.5% only. However, very negligible amount of Cu (below 2 ppb) was detected by ICP, during first, second, third and fourth time of reuse. This result was indicate true heterogeneous nature of the catalyst.

Influence of reaction parameters

Role of support was studied to access the role of surface basicity in selective hydrogenation of cinnamaldehyde to cinnamyl alcohol and the activity data is shown in Figure 8a. Acidic support such as ZrO₂ shows poor hydrogenation activity (Figure 8a); whereas binary oxides with acid-base property like Ln₂O₃, ZnO Al₂O₃ shows high activity compare to acidic supports. While, in case of Al₂O₃ (better known as amphoteric support) shows only 11.7% cinnamaldehyde conversion. This may be because of the presence of γ - phase; which gives the catalyst additional surface acidity causes rendering the catalyst activity. However, Cu-MgO catalyst (prepared by sonochemical method) shows 97.2% cinnamaldehyde conversion with 100% product selectivity. In next, we have collected the reaction product in regular interval (every 1h), in order to check the influence of time-on-stream on the cinnamaldehyde conversion and cinnamyl alcohol selectivity. The results shows (Figure 8b) linear trend of cinnamaldehyde conversion and cinnamyl alcohol selectivity till 7h. Above 7h, though the conversion upsurge to 99% but selectivity gone down as some C=C bond hydrogenation took place. Increasing the amount of reactants affects lowering in amount of product formed, while opposite has been noticed in case of amount of catalyst (Figure 8c). Amount of Cu loading shows seems regular effect on activity and selectivity. The H₂ pulse chemisorption, (expressed in supporting information) to determine the Cu dispersion shown volcanic trend (Figure S6) with the Cu loading. Thereby, because of the high Cu surface coverage; 5%Cu-MgO catalyst shown the best result in our reaction condition.

Hydrogenation of different α,β -unsaturated compounds

The reactivity of different α,β unsaturated compounds for the selective reduction of $>\text{C}=\text{O}$ group is shown in (Table 4). It was observed that Cu-MgO catalyst showed $>97\%$ conversion for all the substrates tested except aliphatic aldehydes (entry 5,6,7,8 and 11, Table 4). All the aliphatic aldehydes showed $>98\%$ conversion but the selectivity for the corresponding unsaturated alcohols were less compare to other alcohols production. Reduction of crotonaldehyde produce crotyl alcohol with selectivity of 78% (entry 11) and the reduction of trans citral produces the corresponding unsaturated alcohol with selectivity of 68 % (entry 12). The conversion of aromatic

ketones and nitro phenol (entry 9,10) was less than other aldehydes. Thereby, the loss in chemoselectivity selectivity over Cu-MgO particularly in case of aliphatic aldehydes is likely controlled by the significantly higher activation barriers to hydrogenate the C=O bond compared with those require for the hydrogenation of C=C bond⁴⁵. According to the theoretical studies reported by Goyal *et al.* it was observed that the aldehyde carbon (C=O) has the highest electrophilicity (0.177), compare to the the second most electrophilic centre, one of the C=C carbons (0.177).⁴⁶ This explains why the hydrogenation is selective and faster through C=O than through other possible centres in our system. The Cu-nanoclusters supported on nanocrystalline MgO (Cu/MgO) catalyst showed very high activity and selectivity compared to impregnated and co-precipitation catalyst, indicated that the conversion activity and selectivity of the catalyst depends on the size of the Cu-nanoclusters, nanocrystalline support and highly dispersion nature of the Cu-species.

Possible mechanisms of catalytic hydrogen transfer reactions

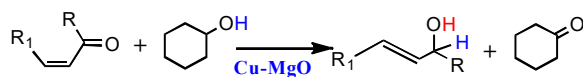
Hydrogen transfer reaction of α , β unsaturated carbonyl compounds are believed to occur according to the Meerwein-Ponndorf-verley (MPV) mechanism C=O bond of the unsaturated carbonyl will have interaction with weak Lewis acid Mg^{+2} cation and Cu^0 atom with simultaneous non-dissociative cyclohexanol adsorption on Mg^{+2} and Cu^0 giving rise to a cyclic 6 atom surface intermediate.⁴⁷⁻⁴⁹

Conclusions

In conclusion, we have prepared Cu-nanoclusters supported on nanocrystalline MgO and found that this catalyst is highly active for the simultaneous dehydrogenation of cyclohexanol to produce cyclohexanone and selective hydrogenation of hydrogenation of α,β unsaturated carbonyl compounds to produce corresponding α , β unsaturated alcohols. Presence of highly dispersed, small metallic Cu particles found to be the key factor for chemoselective hydrogenation of α,β unsaturated carbonyl compounds. This Cu-MgO catalyst can be reuse at least five times without any activity loss confirming the true heterogeneity of the catalyst.

Acknowledgements

R. B. thanks CSIR, New Delhi for the financial support in the form of the 12 FFYP (CSC-0117 and CSC-0125). We also acknowledge Director CSIR-IIP for his support. The authors thank Analytical Science Division, CSIR-Indian Institute of Petroleum for analytical services. EXAFS measurements were performed at KEK-IMSS-PF TSukuba, Japan with the approval of Photon Factory Advisory committee (Project 2014 6070 and 2015 6712).



Scheme 1. Schematic of selective transfer hydrogenation of α,β -unsaturated carbonyl compounds.

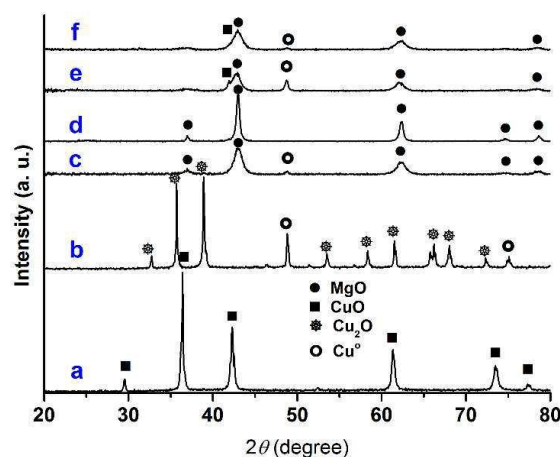


Figure 1. X-ray diffraction pattern of (a) CuO; (b) Cu₂O; (c) MgO; (d) 5%Cu-MgOcom; (e) 5%Cu-MgO and (f) 5%Cu-MgOused.

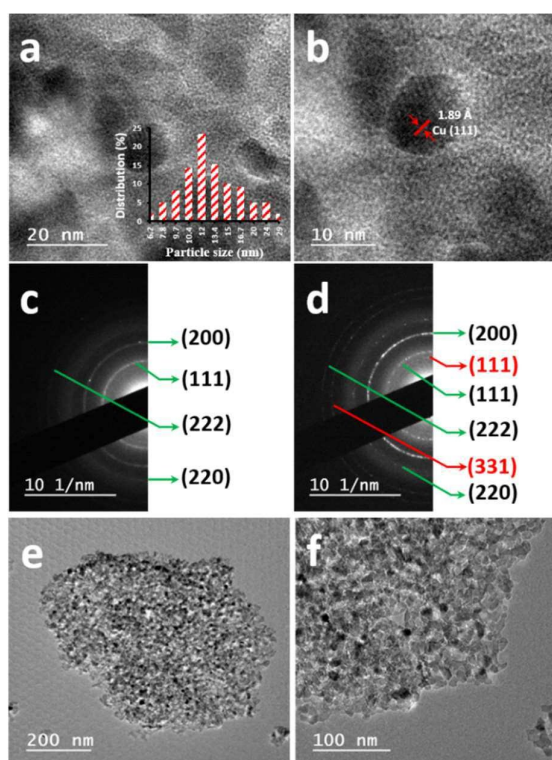


Figure 2. Typical TEM images for 5%Cu-MgO catalyst, the Inter-planer spacing has been indexed as per JCPDS card no 04-0836.

ARTICLE

Journal Name

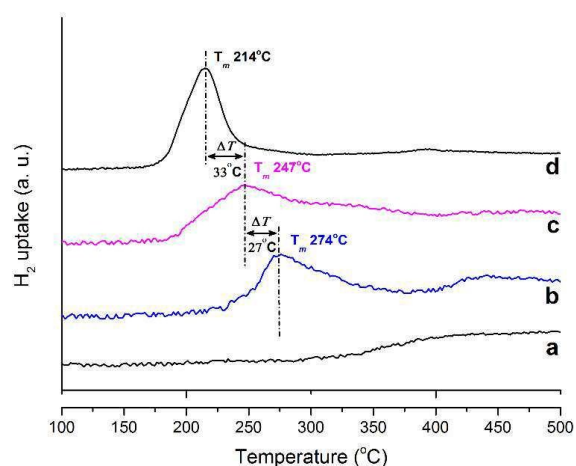


Figure 3. TPR patterns of calcined catalysts: (a) MgO, (b) 5%Cu-MgO impregnated (c) 5%Cu-MgO with hydrazine & 3h without sonication and (d) 5%Cu-MgO with hydrazine and 3h sonication.

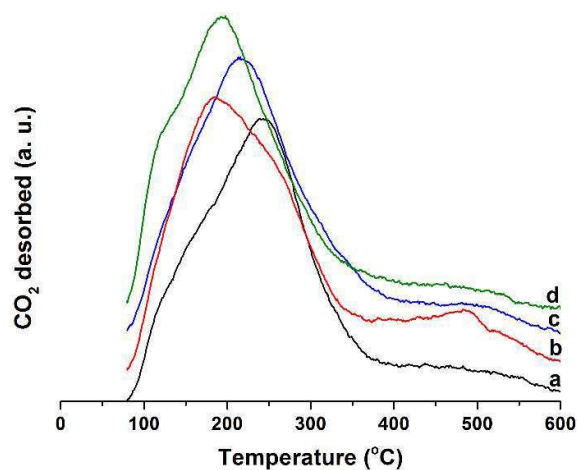


Figure 4. CO₂-TPD profile of (a) MgO, (b) 2.5%Cu-MgO, (c) 5%Cu-MgO and (d) 10%Cu-MgO catalyst.

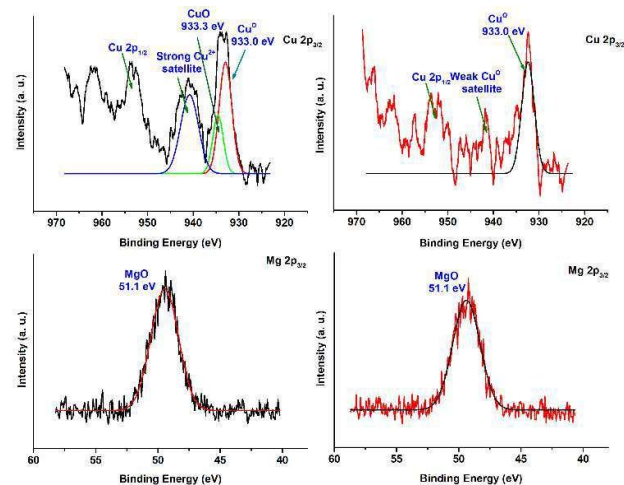


Figure 5. XP spectra of Cu 2p and Mg 2p of the 5%Cu-MgO catalyst. (black: fresh catalyst and red: spent catalyst)

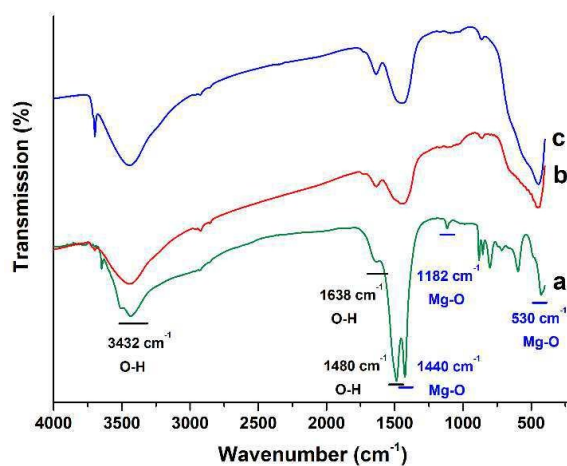


Figure 6. FT-IR spectra of Cu-MgO catalyst (a) 5%Cu-MgO uncalcined, (b) 5%Cu-MgO calcined and (c) 5%Cu-MgONH calcined.

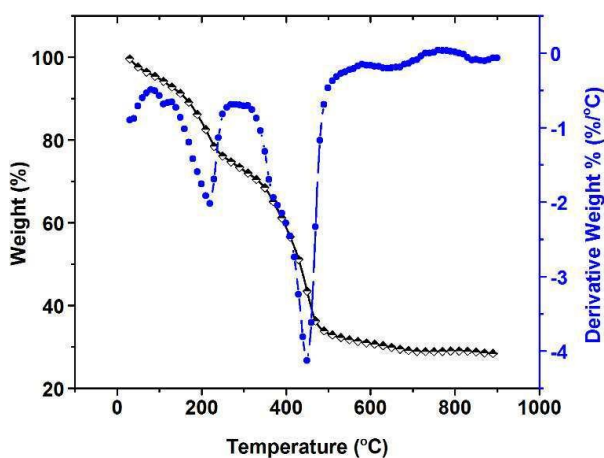


Figure 7. TGA of uncalcined 5%Cu-MgO catalyst.

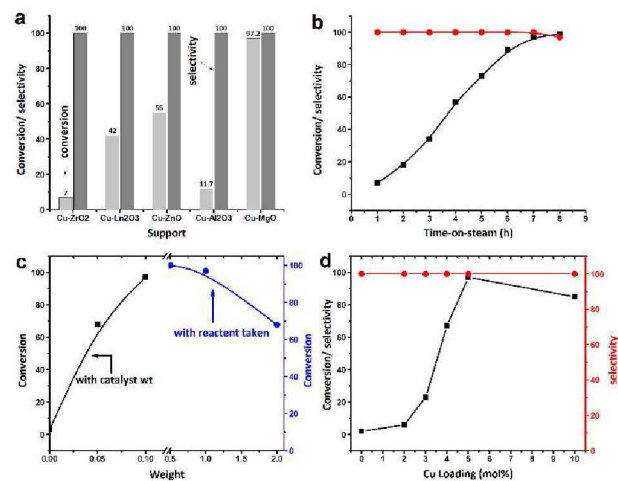
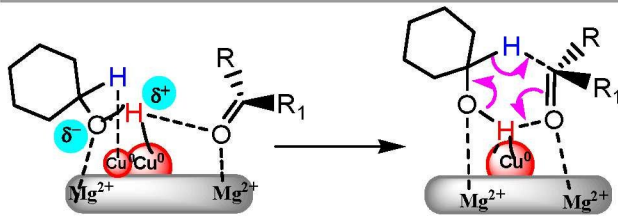


Figure 8. Activity and selectivity of cinnamaldehyde hydrogenation with (a) different support; (b) time-on-steam; (c) weight of catalyst (in black square) and reactant (in round blue) taken and (d) Cu loading.

Condition: 1 g of substrate, 20 ml of cyclohexanol, 0.1 g catalysts, 1 MPa N₂ and 180°C.



Scheme 2. Possible reaction mechanism for selective transfer hydrogenation of α,β -unsaturated carbonyl compounds over Cu-MgO catalyst.

Table 1. Physicochemical properties of the catalyst

Catalyst	BET Surface area m ² /g	Cu Dispersion (%)	Cu specific surface area/m ² g	Basicity mmol/g
MgO	107	-	-	1.346
2.5%Cu-MgO	132	27.5	186.5	1.127
5%Cu-MgO	104.9	49.7	336.6	0.9601
10%Cu-MgO	97.8	20	136.7	0.753
5%Cu-MgO ^{imp}	37.7	11.4	77.2	-
5%Cu-MgO ^{co-pre}	58.1	07.2	29.8	-

^a Physically mixed catalyst.

Table 2. Summary of the EXAFS fitting results for the fresh and spent Cu catalysts^a

	Path	R (10 ⁻¹ nm)	CN	DW (10 ⁻⁵ nm ²)	ΔE_0 (eV)	R _f (%)
Fresh	Cu-O	1.958±0.012	2.0±0.4	1.8±1.7	-5.0±2.9	1.2
Spent	Cu-O	1.932±0.032	0.6±0.7	0.6±6.3	-11.2±3.7	8.6
	Cu-Cu	2.553±0.023	8.3±2.9	15.3±3.1		

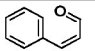
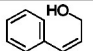
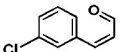
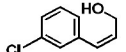
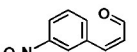
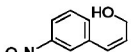
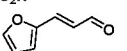
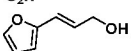
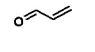
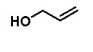
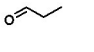
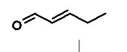
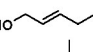
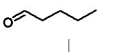
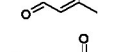
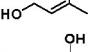
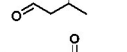
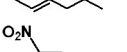
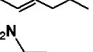
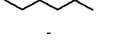
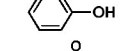
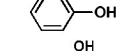
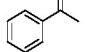
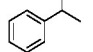
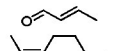
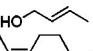
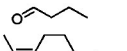
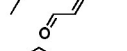
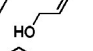
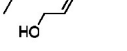
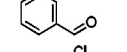
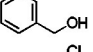
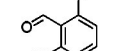
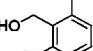
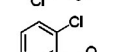
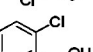
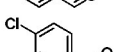
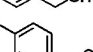
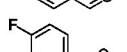
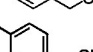
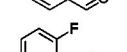
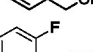
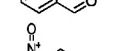
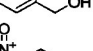
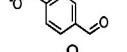
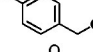
^a Fitting was conducted in the range Δk : 3–13 (10⁻¹ nm) and ΔR : 1.2–2.8 (10⁻¹ nm). Amplitude reducing factor S₀² was set as 0.95

Table 3. Activities of hydrogenation of cinnamaldehyde over different H₂ donor.

SI No	Substrate (7.34mmol)	H ₂ donor	Amount of RC=O (mmol)	r _{temp}	r _{time}	χ_c	χ_s
							C-OH
1			5.3	180	7	61.8	 100
2			4.5	180	7	55.0	 100
3			7.8	100	7	97.2	 100
4			0.92	180	7	11.6	 100

Reaction conditions: 1 g of substrate, 20 ml of each alcohol, 0.1 g catalysts, 1 MPa N₂ and 180°C; conversion and product selectivity in mole %; χ_c : hydrogenation of cinnamaldehyde; χ_s : product selectivity. R-C=O (mmol)= initial amount (mmol) of cyclohexanol-after reaction cyclohexanol amount (mmol)/ initial amount (mmol) of cyclohexanol

Table 4. Activities of Cu-MgO catalyst on different α,β -unsaturated carbonyl compounds.

Sl. No	Substrate	χ^C	χ^S				TOF (h^{-1})	H_2 efficiency (mmol)
			C-OH	Sel.	C=O	Sel.		
1		97.2		100	-	-	13.31	7.8
2		97		100	-	-	10.60	7.8
3		97		100	-	-	9.94	7.8
4		97		100	-	-	21.29	7.8
5		98		77		23	31.75	8.1
6		98.6		75		25	21.29	8.0
7		98.8		85		15	21.33	8.0
8		48		43		57	8.88	5.6
9		46		100	-	-	5.99	5.6
10		35		100	-	-	5.28	5.2
11		98.1		78		22	25.42	8.1
12		98.7		68		32	11.76	8.1
13		99.0		100	-	-	16.93	8.2
14		99.6		100	-	-	10.32	8.0
15		99.3		100	-	-	12.82	8.0
16		99.0		100	-	-	12.78	8.0
17		99.1		100	-	-	14.48	8.0
18		99.4		100	-	-	14.53	8.0
19		99.7		100	-	-	11.96	8.1
20		99.7		100	-	-	11.96	8.1

Reaction conditions: 1 g of substrate, 20 ml of cyclohexanol, 0.1 g catalysts, 1 MPa N_2 and 180°C; conversion and product selectivity in mole %; χ^C : conversion of different α,β -unsaturated carbonyl compounds; χ^S : product selectivity.

References

- M. Zhao, K. Yuan, Y. Wang, G. Li, J. Guo, L. Gu, W. Hu, H. Zhao and Z. Tang, *Nature*, 2016, **539**, 76-80.
- B. Ding, Z. Zhang, Y. Liu, M. Sugiya, T. Imamoto and W. Zhang, *Org. Lett.*, 2013, **15**, 3690-3693.
- N. J. A. Martin and B. List, *J. Am. Chem. Soc.*, 2006, **128**, 13368-13369.
- M. B. Smith and J. March, *March's advanced organic chemistry: reactions, mechanisms, and structure*, John Wiley & Sons, 2007.
- R. L. Augustine, *Catalytic Hydrogenation: Techniques and Applications in Organic Synthesis*, Marcel Dekker, Incorporated, 1965.
- G. C. Bond, *Catalysis by metals*, Academic Press, 1962.
- V. Gutierrez, M. Alvarez and M. A. Volpe, *Applied Catalysis A: General*, 2012, **413**, 358-365.
- S. Handjani, E. Marceau, J. Blanchard, J.-M. Krafft, M. Che, P. Mäki-Arvela, N. Kumar, J. Wärnå and D. Y. Murzin, *J. Catal.*, 2011, **282**, 228-236.

9. M. A. Aramendía, V. Borau, C. Jiménez, J. M. Marinas, A. Porras and F. J. Urbano, *J. Catal.*, 1997, **172**, 46-54.
10. P. Mäki-Arvela, J. Hájek, T. Salmi and D. Y. Murzin, *Applied Catalysis A: General*, 2005, **292**, 1-49.
11. A. Vicente, T. Ekou, G. Lafaye, C. Especel, P. Marécot and C. T. Williams, *J. Catal.*, 2010, **275**, 202-210.
12. P. Reyes, H. Rojas and J. L. G. Fierro, *Applied Catalysis A: General*, 2003, **248**, 59-65.
13. F.-X. Legrand, F. Hapiot, S. Tilloy, A. Guerriero, M. Peruzzini, L. Gonsalvi and E. Monflier, *Applied Catalysis A: General*, 2009, **362**, 62-66.
14. C. Tsai-Chin, L. Hsin-Yi, L. Pei-Hua, C. Jiunn-Hsing and L. Chiu-Hsun, *Nanotechnology*, 2013, **24**, 115601.
15. N. Mahata, F. Gonçalves, M. F. R. Pereira and J. L. Figueiredo, *Applied Catalysis A: General*, 2008, **339**, 159-168.
16. M. B. Padley, C. H. Rochester, G. J. Hutchings and F. King, *J. Catal.*, 1994, **148**, 438-452.
17. B. Bridier, N. López and J. Pérez-Ramírez, *J. Catal.*, 2010, **269**, 80-92.
18. E. Simón, J. M. Rosas, A. Santos and A. Romero, *Catal. Today*, 2012, **187**, 150-158.
19. N. Ravasio, F. Zaccheria, M. Gargano, S. Recchia, A. Fusi, N. Poli and R. Psaro, *Applied Catalysis A: General*, 2002, **233**, 1-6.
20. D. Scholz, C. Aellig and I. Hermans, *ChemSusChem*, 2014, **7**, 268-275.
21. T. S. Hansen, K. Barta, P. T. Anastas, P. C. Ford and A. Riisager, *Green Chem.*, 2012, **14**, 2457-2461.
22. Y. Yuan, S. Yao, M. Wang, S. Lou and N. Yan, *Curr. Org. Chem.*, 2013, **17**, 400-413.
23. M. Steffan, A. Jakob, P. Claus and H. Lang, *Catal. Commun.*, 2009, **10**, 437-441.
24. J. Zhao, H. Chen, J. Xu and J. Shen, *J. Phys. Chem. C*, 2013, **117**, 10573-10580.
25. E. Stern, M. Newville, B. Ravel, Y. Yacoby and D. Haskel, *Physica B: Condensed Matter*, 1995, **208**, 117-120.
26. M. Newville, P. Liviņš, S. Y. Yacoby, J. Rehr and E. Stern, *Phys. Rev. B*, 1993, **47**, 14126.
27. A. Ankudinov, B. Ravel, J. Rehr and S. Conradson, *Phys. Rev. B*, 1998, **58**, 7565.
28. A. Ankudinov, A. Nesvizhskii and J. Rehr, *Phys. Rev. B*, 2003, **67**, 115120.
29. B. Ravel, *Journal of synchrotron radiation*, 2001, **8**, 314-316.
30. S. A. Carabineiro, N. Bogdanchikova, A. Pestryakov, P. B. Tavares, L. S. Fernandes and J. L. Figueiredo, *Nanoscale research letters*, 2011, **6**, 1-6.
31. S. Elzey, J. Baltrusaitis, S. Bian and V. H. Grassian, *J. Mater. Chem.*, 2011, **21**, 3162-3169.
32. B. Sarkar, R. Goyal, C. Pendem, T. Sasaki and R. Bal, *J. Mol. Catal. A: Chem.*, 2016, **424**, 17-26.
33. M. S. El-Eskandarany, M. Omori, T. Hirai, T. Konno, K. Sumiyama and K. Suzuki, *Metallurgical and Materials Transactions A*, 2001, **32**, 157-164.
34. R. Tiwari, B. Sarkar, R. Tiwari, C. Pendem, T. Sasaki, S. Saran and R. Bal, *J. Mol. Catal. A: Chem.*, 2014, **395**, 117-123.
35. B. Sarkar, C. Pendem, L. S. Konathala, R. Tiwari, T. Sasaki and R. Bal, *Chem. Commun.*, 2014, **50**, 9707-9710.
36. B. Sarkar, P. Prajapati, R. Tiwari, R. Tiwari, S. Ghosh, S. S. Acharyya, C. Pendem, R. K. Singha, L. S. Konathala and J. Kumar, *Green Chem.*, 2012, **14**, 2600-2606.
37. S. Bennici and A. Auroux, in *Metal Oxide Catalysis*, Wiley-VCH Verlag GmbH & Co. KGaA, 2009, DOI: 10.1002/9783527626113.ch9, pp. 391-441.
38. C. D. Wagner and G. Muilenberg, *Handbook of X-ray photoelectron spectroscopy*, Perkin-Elmer, 1979.
39. L. Ai, H. Yue and J. Jiang, *Nanoscale*, 2012, **4**, 5401-5408.
40. M. B. Gawande, P. S. Branco, K. Parghi, J. J. Shrikhande, R. K. Pandey, C. Ghumman, N. Bundaleski, O. Teodoro and R. V. Jayaram, *Catalysis Science & Technology*, 2011, **1**, 1653-1664.
41. B. Sarkar, R. K. Singha, R. Tiwari, S. Ghosh, S. S. Acharyya, C. Pendem, L. N. S. Konathala and R. Bal, *RSC Adv.*, 2014, **4**, 5453-5456.
42. F. Zhang, R. Zhang, J. Feng, L. Ci, S. Xiong, J. Yang, Y. Qian and L. Li, *Nanoscale*, 2015, **7**, 232-239.
43. G. Brieger and T. J. Nestruck, *Chem. Rev.*, 1974, **74**, 567-580.
44. N. Weinberg and H. Weinberg, *Chem. Rev.*, 1968, **68**, 449-523.
45. M. S. Ide, B. Hao, M. Neurock and R. J. Davis, *ACS Catalysis*, 2012, **2**, 671-683.
46. R. Goyal, B. Sarkar, A. Bag, N. Siddiqui, D. Dumbre, N. Lucas, S. K. Bhargava and A. Bordoloi, *J. Catal.*, 2016, **340**, 248-260.
47. F. Braun and J. Di Cosimo, *Catal. Today*, 2006, **116**, 206-215.
48. M. a. A. Aramendía, V. Borau, C. Jiménez, J. M. Marinas, J. R. Ruiz and F. J. Urbano, *Applied Catalysis A: General*, 2003, **244**, 207-215.
49. J. Ramos, V. Díez, C. Ferretti, P. Torresi, C. Apesteguía and J. Di Cosimo, *Catal. Today*, 2011, **172**, 41-47.

Graphical Abstract

